MEDICAL SCIENCE MONITOR

CLINICAL RESEARCH

e-ISSN 1643-3750
© Med Sci Monit, 2019; 25: 2505-2510
DOI: 10.12659/MSM.913110

Received: 2018.09.08
Accepted: 2018.11.29
Published: 2019.04.05

The Role of Tumor Oxygenation Tested by Magnetic Resonance Imaging (MRI) in Prostate Cancer Grading

Authors' Contribution:
Study Design A
Data Collection B
Statistical Analysis C
Data Interpretation D
Manuscript Preparation E
Literature Search F
Funds Collection G

BC 1 Huaizhen Geng
AD 2 Wen Tong
E 3 Fangzheng Han
DG 4 Kunming Zhu
BF 5 Yumei Cao
AE 6 Xiude Chen

1 Department of Urology, Heze Municipal Hospital, Heze, Shandong, P.R. China
2 Department of Intensive Care Unit (ICU), Heze Municipal Hospital, Heze, Shandong, P.R. China
3 Department of Pathology, Heze Municipal Hospital, Heze, Shandong, P.R. China
4 Department of Radiology, Heze Municipal Hospital, Heze, Shandong, P.R. China
5 Department of Cardiac Intervention, Heze Municipal Hospital, Heze, Shandong, P.R. China
6 Department of Urology, Provincial Hospital Affiliated to Shandong University, Ji'nan, Shandong, P.R. China

Corresponding Author: Xiude Chen, e-mail: mw4441iguw818630@126.com
Source of support: This work was supported by The Natural Science Foundation of China (NO.81202016)

Background: Prostate cancer is a common malignant tumor in males. Prostate cancer grading is an important basis for evaluation of invasion. The purpose of this article was to use dynamic enhanced scan magnetic resonance imaging (MRI) to quantitatively investigate the relationship between tumor oxygenation value and prostate cancer pathological Gleason score.

Material/Methods: A total of 312 prostate cancer patients diagnosed by needle biopsy who received MRI dynamic enhanced scan were enrolled in this study. Multiparameter oxygen concentration image based on MRI was applied to test pO2 in tumors. Multiple spin resonance image relaxation time edit sequence and weak field diffusion model were used to estimate oxygen saturation level and pO2. hematoxylin and eosin staining and Gleason score were used to determine biological behavior and prognosis.

Results: According to the Gleason score system, there were 28 cases with a score of 10, 112 cases with a score of 9, 56 cases with a score of 8, and 116 cases with a score lower than 7. The enrolled patients were divided into groups: 116 cases into the middle-to-well differentiation group (Gleason score ≤7) and 196 cases into the poorly differentiation group (Gleason score at 8 to 10). Prostate cancer tumor oxygenation value was positively correlated with Gleason score (r=0.349, *P*<0.05) or PSA (r=0.432, *P*<0.05). Tumor oxygenation value in Gleason ≤7 group was obviously different from that in the group with Gleason score between 9 and 10 (*P*<0.05).

Conclusions: Tumor oxygenation value in prostate cancer was positively correlated with Gleason score. Tumor oxygenation value might be useful in clinics to evaluate prostate cancer grading and prognosis.

MeSH Keywords: **Magnetic Resonance Imaging • Neoplasm Grading • Prostatic Neoplasms**

Full-text PDF: https://www.medscimonit.com/abstract/index/idArt/913110

1922 5 4 29

Indexed in: [Current Contents/Clinical Medicine] [SCI Expanded] [ISI Alerting System] [ISI Journals Master List] [Index Medicus/MEDLINE] [EMBASE/Excerpta Medica] [Chemical Abstracts/CAS]

Background

Prostate cancer is a common male reproductive system malignant tumor worldwide. As populations age and lifestyles change, prostate cancer morbidity and mortality has shown a rising trend that seriously threatens the health and well-being of many people [1,2]. Prostate cancer treatment often is administered according to the cancer degree and grading [3]. Gleason grading is currently the most widely used method. Many patients receive a clear pathological grading after application of Gleason score in evaluating prostate cancer. Gleason grading has become the standard of evaluating prostate cancer invasion [4,5]. Currently, ultrasound combined with prostate biopsy is not only used for diagnosis, but also for pathological grading. However, how best to combine ultrasound and Gleason grading together to evaluate prostate cancer diagnosis and prognosis is still unclear [6].

Dynamic enhanced scan magnetic resonance imaging (MRI) is widely used in clinics especially for tumor detection, location, and prognosis evaluation. Moreover, MRI can be used for tumor grading [7,8]. Previous studies have indicated that MRI can detect contrast agent distribution in different tissues and organs. It can distinguish malignant and benign tumors, and provide a new noninvasive method for tumor diagnosis [9,10]. Although contrast agent toxicity generally has a small incidence rate, it often causes a variety of clinical complications such as sepsis and infection [11]. Thus, research to find a better way without invasion and clinical complications is needed.

It is well known that the tumor microenvironment is a hypoxia environment, while the oxygen content in normal tissues and organs is relatively definite [12]. We aimed to explore how best to use MRI combined with tumor oxygenation for prostate cancer diagnosis and pathology grading.

This article applied MRI combined with tumor oxygenation to evaluate prostate cancer grading and prognosis. We performed prostate periphery dynamic MRI scans to quantitatively determine tumor oxygenation values and explore its correlation with Gleason score. This study will provide a basis for the relationship between noninvasively evaluation of the biological invasion of prostate cancer and pathological Gleason score for use in clinics.

Material and Methods

Object of study

A total of 312 cases of prostate cancer patients diagnosed by needle biopsy who had received MRI dynamic enhanced scan were enrolled in this study. The age of patients was 43–81years old (70.3±7.2 years old), and serum PSA content was 2.6–1562.0 ng/L. Inclusion criteria of this study were as follows [13,14]: 1) patients diagnosed by needle biopsy with complete pathology and related information. 2) Patients received MRI dynamic enhanced scan with complete information. 3) No patients received surgery, immune therapy, radiotherapy, or chemotherapy before needle biopsy and MRI scan. 4) The time interval between MRI scan and surgery or biopsy was less than 30 days. Exclusion criteria [13,14] included: 1) incomplete pathological information; 2) incomplete scanning information; 3) patients received surgery, immune therapy, radiotherapy, or chemotherapy before needle biopsy and MRI scan; and 4) the time interval between MRI scan and surgery or biopsy was longer than 30 days.

MRI

MRI scan was performed using a routine method [15,16]. Patients received fluid and laxative to keep intestinal tract clean. MRI scan was performed on GE 1.5T and 5.0T Signa Twin Speed scanner. Phased-array coil with 16 channels were applied. In order to reduce the influence of breathing, the scanning coil was fixed by binding. Specific scanning sequence was as follows: 1) local prostate gland axis (T1WI) scan parameter: layer thickness 6 mm, TR 460 ms, scanning twist angle 5°, TE 16 ms, interlamellar scanning spacing 0.6 mm, FOV 25×25 cm, NEX 2, matrix 125×256. 2) Coronary pressure fast spin resonance and local prostate gland axis scanning parameter: TR 3600 ms, scan echo chain length 20, scanning thickness 6 mm, TE 88 ms, interlamellar scanning spacing 0.6 mm, scanning view 36×36 cm, NEX 8, matrix 256×128. 3) Scanning parameters from the median sagittal echo or abdominal aortic bifurcation horizontal axis to the base of the prostate: FOV 30×48 cm, NEX 2, TR 480–560 ms, interlamellar scanning spacing 2–4 mm, TE 16 ms, scanning thickness 6–10 mm, matrix 128×256.

Prostate local dynamic enhanced MRI scanning process [17,18] was as follows: gadolinium-diethylenetriamine pentaacetic acid (Gd-DTPA) as a contrast agent was injected to the patients through elbow vein at 0.1 mmol/L and the injection speed was 3.0–4.0 mL/sec. Another 20 mL normal saline was continued injected after contrast agent injection to flush the vein. A set of scans was performed for continuous 16 cycles as control before contrast agent injection. Dynamic enhanced MRI scan parameters were as follows: scanning layer thickness 3.8 mm, TE 2.0 ms, interlamellar scanning spacing 2.0 mm, FOV 40×48 cm, TR 5 ms, matrix 128×512. Each patient had 30 dynamic processes and 60 images in each dynamic scanning process.

Prostate needle biopsy

According to a routine method [19,20], prostate needle biopsy was performed under transrectal ultrasonography guidance. The prostate was routinely tested at first, based on size and the 8 zones method (8–16 needles). Doubtful procedures required

Indexed in: [Current Contents/Clinical Medicine] [SCI Expanded] [ISI Alerting System] [ISI Journals Master List] [Index Medicus/MEDLINE] [EMBASE/Excerpta Medica] [Chemical Abstracts/CAS]

Table 1. Prostate cancer needle biopsy pathological score.

Gleason score	≤7	8	9	10	Total
Cases	116	56	112	28	312
Percentage	37.2%	17.9%	35.9%	9.0%	100%

Table 2. Prostate cancer needle biopsy pathological grouping.

Group	Middle to well differentiation group	Poorly differentiation group	Total
Cases	116	196	318
Percentage	37.2%	62.8%	100%

another targeted puncture for 2–6 needles. The biopsy tissue was fixed in 10% formaldehyde solution and used for hematoxylin and eosin staining [21]. Gleason score was evaluated based on these results. Prostate cancer tissue structure grading was analyzed for 2 parts as 0–10.

MRI scanning image analysis

MRI scanning image was analyzed by tumor oxygenation computing system under MATLAB R2009a (Frontier Interdisciplinary Research Institute of Beijing University). DCE-MRI information and data were input to the system and tumor oxygenation value of target area was calculated [22]. Average tumor oxygenation value, ROI tumor oxygenation pseudo color map, gray-time curve, mean Kep value, and contrast vessel time-concentration curve of selected area were analyzed.

Statistical analysis

All data were analyzed on SPSS16.0 software. Numerical variables were presented as mean ± standard deviation. Gleason scores and tumor oxygenation value comparison were performed by one-way ANOVA. The correlation relationship between Gleason scores and tumor oxygenation value was analyzed by Spearman correlation analysis. $P<0.05$ was considered as statistical significance.

Results

Needle biopsy pathological results

A total of 312 cases of prostate cancer patients were enrolled in this study. As shown in Table 1, according to the Gleason score system, there were 28 cases with score 10, 112 cases with score 9, 56 cases with score 8, and 116 cases with a score lower than 7. The enrolled patients were divided into middle-to-well differentiation group (Gleason score ≤7) (n=116) and poorly differentiation group (Gleason score at 8–10) (n=196) (Table 2).

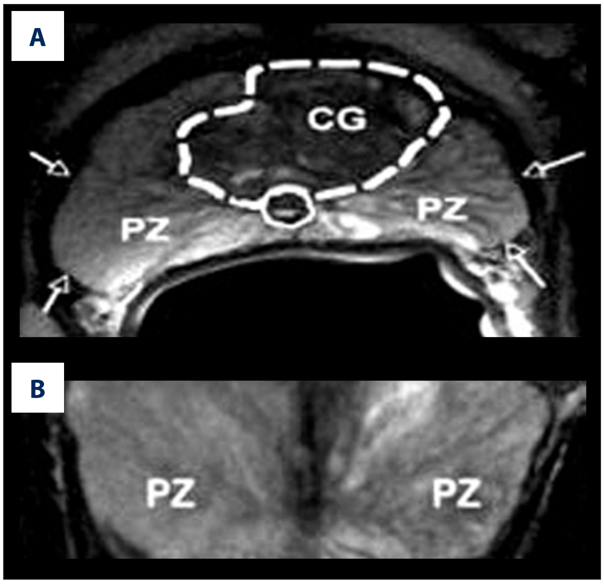

Figure 1. (**A, B**) Healthy volunteer prostate scanning image.

MRI scanning case result

A 60-year-old male healthy volunteer underwent prostate MRI scan and showed high signal intensity in peripheral zone (PZ) in an axial T2 weighted image (prostate cross section) (Figure 1A). The signal strength in central gland (CG; dotted line) was lower than peripheral zone (PZ). Prostate capsule (arrow) was clearly found. Regarding Coronal T2W image through prostate (Figure 1B), PZ was surrounded by distal prostatic urethra and ejaculatory duct. Seminal vesicle was the tubular structure (SV) with high signal intensity and full of liquid.

In terms of patients with prostate cancer, T3 prostate cancer scanning was performed in peripheral zone. T2 weighted (Figure 2A) axial image and coronal plane (Figure 2B) image revealed low intensity tumor signal in left peripheral zone (arrow). Tumor nodule produced swell and irregular capsule, suggesting that patient in penetration period.

Indexed in: [Current Contents/Clinical Medicine] [SCI Expanded] [ISI Alerting System] [ISI Journals Master List] [Index Medicus/MEDLINE] [EMBASE/Excerpta Medica] [Chemical Abstracts/CAS]

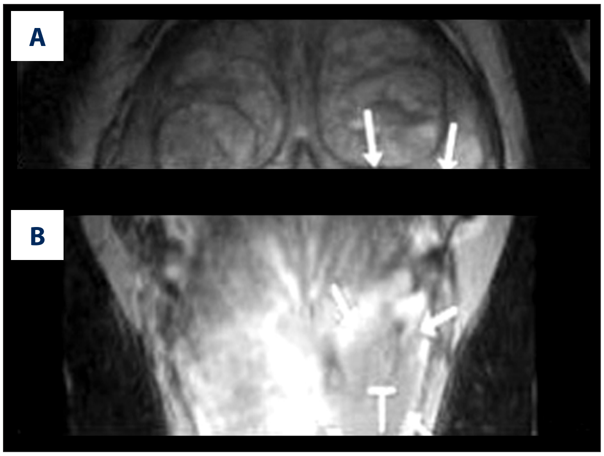

Figure 2. (**A, B**) Prostate cancer patient prostate scanning image.

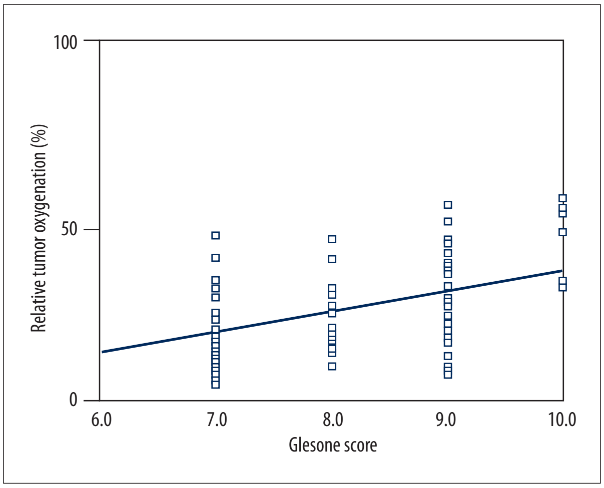

Figure 3. Magnetic resonance imaging scan tumor oxygenation value comparison between different Gleason score.

MRI scan tumor oxygenation value comparison between different Gleason score

Figure 3 shows MRI scans and tumor oxygenation value of the different Gleason score groups. Following the improvement of Gleason score, tumor oxygenation value presented an increasing trend. Tumor oxygenation value showed significant differences among groups (F=2.928, $P<0.05$) (Figure 3). Obvious characteristics was observed among different Gleason score groups: tumor oxygenation value in Gleason score ≤7 group was markedly different from that in Gleason score 9–10 group ($P<0.05$). However, no significant difference was observed among Gleason score ≤7, score 8, score 9, and score 10 ($P>0.05$).

Table 4. MRI tumor oxygenation value.

Gleason score	MR tumor oxygenation value
≤7	$1.02\pm0.16\times10^{-3}$ mm^2
8	$0.86\pm0.05\times10^{-3}$ mm^2
9	$0.63\pm0.17\times10^{-3}$ mm^2
10	$0.43\pm0.04\times10^{-3}$ mm^2

Table 5. Correlation analysis of MRI dynamic enhanced scanning prostate cancer tumor oxygenation value and Gleason score.

Detection method	Gleason score	Accuracy (%)
MRI tumor oxygenation	258/312	82.7
χ^2	9.73	18.88
P	0.043	0.017

Accuracy of MRI tumor oxygenation value on diagnosing prostate cancer

As shown in Table 3, the accuracy of MRI tumor oxygenation value on diagnosing prostate cancer were listed as follows: the accuracy rate of MRI tumor oxygenation value at ≤7, 8, 9, and 10 were 91/116 (78.5%), 47/56 (83.9%), 98/116 (87.5%), and 22/28 (78.6%), respectively with a mean accuracy of 82.3%. Table 4 showed the specific value of MRI tumor oxygenation. The data suggested that MRI tumor oxygenation value may be a potential index for prostate cancer.

Correlation analysis of MRI dynamic enhanced scanning prostate cancer tumor oxygenation value with Gleason score or PSA

Correlation analysis showed a significant correlation of MRI dynamic enhanced scanning prostate cancer tumor oxygenation

Table 3. Accuracy of MRI tumor oxygenation value on diagnosing prostate cancer.

Gleason score	MR tumor oxygenation (cases)				Total	Accuracy (%)
	≤7	8	9	10		
≤7	91/116	0	0	0	116	78.5%
8	0	47/56	0	0	56	83.9%
9	0	0	98/112	0	112	87.5%
10	0	0	0	22/28	28	78.6%

Indexed in: [Current Contents/Clinical Medicine] [SCI Expanded] [ISI Alerting System] [ISI Journals Master List] [Index Medicus/MEDLINE] [EMBASE/Excerpta Medica] [Chemical Abstracts/CAS]

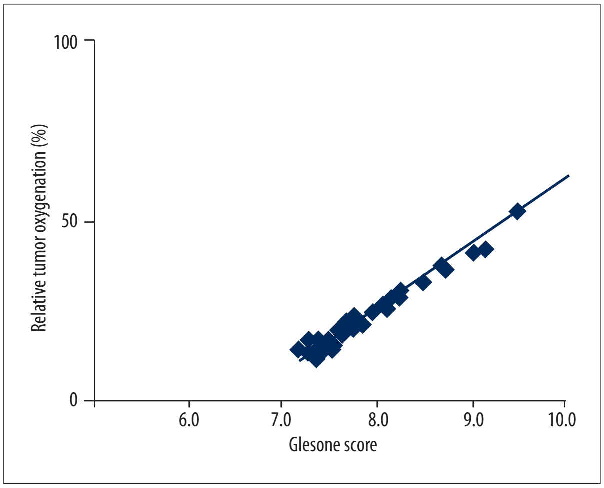

Figure 4. Correlation result of magnetic resonance imaging dynamic enhanced scanning prostate cancer tumor oxygenation value and Gleason score.

value with Gleason score (r=0.342, $P<0.05$) (Table 5, Figure 4). In addition, we also found a correlation of tumor oxygenation value with PSA value (r=0.432, $P<0.05$).

Discussion

Prostate cancer is a seriously threat to men's health and life. Gleason grading has become the standard of evaluating prostate cancer invasion. However, this method requires a biopsy procedure that is tedious and painful [23]. Although MRI is widely used in prostate cancer detection, location, and prognosis evaluation, contrast agents often causes a variety of clinical complications such as sepsis and infection [24]. Thus, there is an urgent need to find a more effective method with fewer side effects for prostate cancer diagnosis and grading.

In this study, we aimed to adopt MRI for prostate cancer diagnosis and grading from tumor oxygenation perspective according to the tumor microenvironment which is a hypoxia environment [25]. This study successfully established multiparameter oxygen concentration images based on MRI and tumor oxygenation. It was found that prostate cancer area tumor oxygenation value was positively correlated with Gleason score, indicating that tumor oxygenation value might be useful in the evaluation of prostate cancer grading and disease prognosis in clinics. However, due to the limited number patients enrolled in our study, a large cohort clinical study is required to confirm the value of tumor oxygenation in assessing the grade and prognosis of prostate cancer.

Previous studies have shown that MRI can quantitatively measure ADC values [26]. Furthermore, research found that ADC value was negatively correlated with the Gleason grade (r=–0.39 for peripheral zone cancer) [27]. Higher ADC values were also found to be associated with lower Gleason grades in the peripheral zone prostate cancers. Both ADC values and tumor volumes were found to significantly predict tumor aggressiveness, specifically in the peripheral zone (area under the curve, 0.78) [27]. indicating ADC values might help to predict prostate cancer, especially for tumors in the peripheral zone, which is consistent with the finding from our present study. The difference, however, is that one is a positive correlation, while the other is a negative correlation. Some studies have shown that the Cho+Cr/Cit ratio in prostate cancer tissue detected by MRI was positively correlated with Gleason score [28,29]. This indicates that following Gleason score elevation, Cho peak enlarged, while Cit peak decreased in prostate cancer area, which further supported our conclusions.

Our study had 3 limitations: 1) the limited sample size, thus a large size trial is needed in the future for validation. 2) We did not analyze Gleason subscore effect, as tumor oxygenation value in patients with Gleason score <7 was small and cannot be detected by MRI. 3) Our method and system were still immature, the feasibility and the accuracy of MRI tumor oxygenation value remains to be further researched.

Conclusions

In conclusion, we found that tumor oxygenation value in prostate cancer patients was positively correlated with Gleason score. Tumor oxygenation value might be useful in clinics to evaluate prostate cancer grading and prognosis.

Conflict of interest

None.

References:

1. Weaver JK, Kim EH, Vetter JM et al: Presence of MRI suspicious lesion predicts Gleason 7 or greater prostate cancer in biopsy naive patients. Urology, 2016; 88: 119–24
2. Tay KJ, Gupta RT, Brown AF et al: Defining the incremental utility of prostate multiparametric magnetic resonance imaging at standard and specialized read in predicting extracapsular extension of prostate cancer. Eur Urol, 2016; 70(2): 211–13
3. Wang YJ, Huang CY, Hou WH et al: The outcome and prognostic factors for lymph node recurrence after node-sparing definitive external beam radiotherapy for localized prostate cancer. World J Surg Oncol, 2015; 13: 312
4. Engelhard K, Kuhn R, Osten A et al: Impact of magnetic resonance imaging-guided prostate biopsy in the supine position on the detection of significant prostate cancer in an inhomogeneous patient cohort. Scand J Urol, 2016; 50(2): 110–15

Indexed in: [Current Contents/Clinical Medicine] [SCI Expanded] [ISI Alerting System] [ISI Journals Master List] [Index Medicus/MEDLINE] [EMBASE/Excerpta Medica] [Chemical Abstracts/CAS]

5. Thompson JE, van Leeuwen PJ, Moses D et al: The diagnostic performance of multiparametric magnetic resonance imaging to detect significant prostate cancer. J Urol, 2016; 195(5): 1428–35
6. Jia JB, Houshyar R, Verma S et al: Prostate cancer on computed tomography: A direct comparison with multi-parametric magnetic resonance imaging and tissue pathology. Eur J Radiol, 2016; 85(1): 261–67
7. Wang S, Fan X, Medved M et al: Arterial input functions (AIFs) measured directly from arteries with low and standard doses of contrast agent, and AIFs derived from reference tissues. Magn Reson Imaging, 2016; 34(2): 197–203
8. Sargos P, Guerif S, Latorzeff I et al: Definition of lymph node areas for radiotherapy of prostate cancer: A critical literature review by the French Genito-Urinary Group and the French Association of Urology (GETUG-AFU). Cancer Treat Rev, 2015; 41: 814–20
9. Nicholson A, Mahon J, Boland A et al: The clinical effectiveness and cost-effectiveness of the PROGENSA(R) prostate cancer antigen 3 assay and the Prostate Health Index in the diagnosis of prostate cancer: A systematic review and economic evaluation. Health Technol Assess, 2015; 19: 1–192
10. Woodrum DA, Kawashima A, Gorny KR, Mynderse LA: Magnetic resonance-guided thermal therapy for localized and recurrent prostate cancer. Magn Reson Imaging Clin N Am, 2015; 23: 607–19
11. Ahmad AE, Finelli A: Should prebiopsy multiparametric magnetic resonance imaging be offered to all biopsy-naive men undergoing prostate biopsy? Eur Urol, 2016; 69(3): 426–27
12. Westphalen AC, Noworolski SM, Harisinghani M et al: High-resolution 3-T endorectal prostate MRI: A multireader study of radiologist preference and perceived interpretive quality of 2D and 3D T2-weighted fast spin-echo MR images. Am J Roentgenol, 2016: 206: 86–91
13. Henderson DR, de Souza NM, Thomas K et al: Nine-year follow-up for a study of diffusion-weighted magnetic resonance imaging in a prospective prostate cancer active surveillance cohort. Eur Urol, 2016; 69(6): 1028–33
14. You JY, Lee HJ, Hwang SI et al: Value of T1/T2-weighted magnetic resonance imaging registration to reduce the postbiopsy hemorrhage effect for prostate cancer localization. Prostate Int, 2015; 3: 80–86
15. Falcinelli L, Palumbo I, Radicchia V et al: Prostate cancer: Contouring target and organs at risk by kilovoltage and megavoltage CT and MRI in patients with and without hip prostheses. Br J Radiol, 2015; 88: 20150509
16. de Cobelli O, Terracciano D, Tagliabue E et al: Predicting pathological features at radical prostatectomy in patients with prostate cancer eligible for active surveillance by multiparametric magnetic resonance imaging. PLoS One, 2015; 10 e0139696
17. Buge F, Chiavassa S, Herve C et al: Preclinical evaluation of intraoperative low-energy photon radiotherapy using spherical applicators in locally advanced prostate cancer. Front Oncol, 2015; 5: 204
18. Paparo F, Massollo M, Rollandi L et al: The clinical role of multimodality imaging in the detection of prostate cancer recurrence after radical prostatectomy and radiation therapy: past, present, and future. Ecancermedicalscience, 2015; 9: 570
19. Dianat SS, Carter HB, Schaeffer EM et al: Association of quantitative magnetic resonance imaging parameters with histological findings from MRI/ultrasound fusion prostate biopsy. Can J Urol, 2015; 22: 7965–72
20. Siversson C, Nordstrom F, Nilsson T et al: Technical note: MRI only prostate radiotherapy planning using the statistical decomposition algorithm. Med Phys, 2015; 42: 6090–97
21. Kitajima K, Hartman RP, Froemming AT et al: Detection of local recurrence of prostate cancer after radical prostatectomy using endorectal coil MRI at 3 T: Addition of DWI and dynamic contrast enhancement to T2-weighted MRI. Am J Roentgenol, 2015; 205: 807–16
22. Giannini V, Mazzetti S, Vignati A et al: A fully automatic computer aided diagnosis system for peripheral zone prostate cancer detection using multi-parametric magnetic resonance imaging. Comput Med Imaging Graph, 2015; 2: 219–26
23. Paydar I, Kim BS, Cyr RA et al: Urethrogram-directed stereotactic body radiation therapy for clinically localized prostate cancer in patients with contraindications to magnetic resonance imaging. Front Oncol, 2015; 5: 194
24. Salamanca-Cardona L, Keshari KR: (13)C-labeled biochemical probes for the study of cancer metabolism with dynamic nuclear polarization-enhanced magnetic resonance imaging. Cancer Metab, 2015; 3: 9
25. Kang MH, Yu YD, Shin HS et al: Difference in the rate of rectal complications following prostate brachytherapy based on the prostate-rectum distance and the prostate longitudinal length among early prostate cancer patients. Korean J Urol, 2015; 56: 637–43
26. Nagarajan R, Iqbal Z, Burns B et al: Accelerated echo planar J-resolved spectroscopic imaging in prostate cancer: A pilot validation of non-linear reconstruction using total variation and maximum entropy. NMR Biomed, 2015; 28: 1366–73
27. Verma S, Rajesh A, Morales H et al: Assessment of aggressiveness of prostate cancer: correlation of apparent diffusion coefficient with histologic grade after radical prostatectomy. Am J Roentgenol, 2011; 196(2): 374–81
28. Garmer M, Busch M, Mateiescu S et al: Accuracy of MRI-targeted in-bore prostate biopsy according to the Gleason score with postprostatectomy histopathologic control-a targeted biopsy-only strategy with limited number of cores. Acad Radiol, 2015; 22: 1409–18
29. Orczyk C, Rosenkrantz AB, Deng FM et al: A prospective comparative analysis of the accuracy of HistoScanning and multiparametric magnetic resonance imaging in the localization of prostate cancer among men undergoing radical prostatectomy. Urol Oncol, 2016; 34(1): 3.e1–8

Indexed in: [Current Contents/Clinical Medicine] [SCI Expanded] [ISI Alerting System] [ISI Journals Master List] [Index Medicus/MEDLINE] [EMBASE/Excerpta Medica] [Chemical Abstracts/CAS]